Research Square

Preprints are preliminary reports that have not undergone peer review.
They should not be considered conclusive, used to inform clinical practice,
or referenced by the media as validated information.

Stage-Dependent Macular Remodeling and Retinal Microvascular Impairment in Idiopathic Epiretinal Membrane

HeJia Huang
Wuhan University of Science and Technology
XiangGui Zhang
General Hospital of Central Theater Command
Ming Yan
ymwork1003@126.com

Wuhan University of Science and Technology
Ya Ye
General Hospital of Central Theater Command
Zhen Huang
General Hospital of Central Theater Command
YanPing Song
General Hospital of Central Theater Command
ShuMin Shen
Wuhan University of Science and Technology
ChenYu Peng
Hubei University of Medicine
Lei Yang
Southern Medical University

Research Article

Keywords: Idiopathic epiretinal membrane, optical coherence tomography angiography, vessel density, foveal avascular zone, visual acuity

Posted Date: November 18th, 2026

DOI: https://doi.org/10.21203/rs.3.rs-11481885/v1

License: This work is licensed under a Creative Commons Attribution 4.0 International License.
Read Full License

Additional Declarations: No competing interests reported.

Abstract

Background

To characterize stage-related macular microvascular and foveal structural changes in idiopathic epiretinal membrane (iERM) and examine their associations with visual acuity.

Methods

This retrospective cross-sectional study included 103 participants (103 eyes): 78 iERM eyes classified as Govetto stages 1–4 (19, 25, 19, and 15 eyes) and 25 healthy control eyes. Central macular thickness (CMT), foveal avascular zone (FAZ) metrics, superficial and deep retinal vessel density (VD), and choroidal VD were measured using optical coherence tomography (OCT) and OCT angiography (OCTA). Mixed-effects models evaluated stage, vascular layer, and interaction effects. Age- and sex-adjusted robust regressions assessed group differences and stage trends. Associations with logMAR best-corrected visual acuity (BCVA) were analyzed using Spearman correlations and adjusted robust regressions with Holm correction.

Results

The stage-by-layer interaction was not significant ($\chi^2 = 7.21$, df = 3, P = 0.065). Compared with controls, superficial and deep VD were lower mainly in stages 3–4. Each stage increase was associated with higher CMT (+ 76.66 μm), lower FAZ perimeter (− 0.232 mm), and lower FAZ circularity (− 0.038). Choroidal VD showed no clear group differences. After adjustment, greater FAZ circularity was associated with better BCVA (β = −0.080 per 0.1; 95% CI, − 0.133 to − 0.027; Holm-adjusted P = 0.029), whereas the deep-VD association was attenuated.

Conclusions

iERM staging is associated with foveal remodeling and mid-to-late retinal VD reduction. FAZ circularity may provide functional information beyond structural staging, whereas layer-specific VD patterns require longitudinal validation.

Background

Idiopathic epiretinal membrane (iERM) is a fibrocellular proliferative disorder arising at the vitreoretinal interface that can cause macular traction, retinal structural distortion, foveal morphological abnormalities, reduced visual acuity, and metamorphopsia. Its prevalence increases with age, and some patients remain relatively stable over long periods. Clarifying the macular structural and microvascular features at different iERM stages, and further determining whether these imaging changes are related to

visual functional impairment, is therefore important for understanding disease heterogeneity and improving clinical imaging assessment[1–3].

With the application of optical coherence tomography (OCT), the assessment of iERM has evolved from simply observing the presence of the membrane to quantitative analysis of central macular thickness, retinal layers, and tractional changes. The staging scheme proposed by Govetto et al., which incorporates the ectopic inner foveal layer (EIFL) into iERM staging, provides a unified standard for comparing different morphological stages[4]. Subsequent studies have shown that the EIFL and disorganization of the retinal inner layers are associated with visual acuity and postoperative visual recovery[5, 6]. Changes such as foveal structural abnormalities also suggest that iERM staging may reflect the extent of macular tissue remodeling[7, 8]. However, structural staging does not fully equate to visual functional impairment; some patients exhibit marked foveal morphological abnormalities, yet the degree of visual decline is not consistent, suggesting that microvascular and functional indicators are still needed to further understand the clinical manifestations of iERM.

Optical coherence tomography angiography (OCTA) provides an important, non-invasive means of assessing the retinal microvasculature and enables quantitative analysis of the superficial and deep capillary plexuses, the foveal avascular zone (FAZ), and vessel density (VD). Previous studies have observed alterations in FAZ area, perimeter, and morphological regularity in iERM eyes, and have reported VD abnormalities in different retinal vascular layers[9–11]. Subsequently, several studies have adopted different grading schemes or preoperative–postoperative designs to analyze the relationships of FAZ and layer-specific VD with iERM severity and surgical changes[12–14]. These studies suggest that iERM-related imaging abnormalities involve not only the retinal structure but may also be accompanied by geometric and density changes in the foveal vascular network. However, the conclusions regarding the affected vascular layers and the direction of indicator changes are not entirely consistent across studies, and stage-specific comparisons covering the full range of Govetto stages 1–4 remain relatively limited.

Studies have begun to examine the relationship between OCTA imaging metrics and visual function. Some studies have shown that FAZ morphology, central macular thickness, and retinal vascular morphological parameters are associated with preoperative or postoperative best-corrected visual acuity (BCVA)[15–17]. Studies incorporating microperimetry further suggest that deep capillary plexus VD may be related to macular sensitivity and postoperative visual acuity[18]. However, other studies have found that some FAZ and macular VD metrics fail to show stable postoperative prognostic value after incorporating clinical factors[19]. It therefore remains unclear which imaging metrics primarily reflect morphological staging and which remain associated with current visual acuity after adjustment for stage in patients spanning the full range of Govetto stages 1–4.

Accordingly, using a single-eye design, the present study compared superficial, deep, and choroidal VD and macular foveal structural metrics between patients with Govetto stage 1–4 iERM and healthy

controls, with particular focus on the stage-related patterns of superficial and deep VD. In addition, using logMAR BCVA as the functional outcome in iERM eyes, we analyzed the associations between the above imaging metrics and current visual function. This study aimed to characterize the stage-related macular structural–microvascular imaging features of iERM and to identify the imaging phenotypes most closely associated with visual impairment, thereby providing a reference for the further functional assessment and clinical management of patients with similar structural stages but differing degrees of visual functional impairment.

Methods

1. Study design

This was a single-center, retrospective, cross-sectional observational study of patients with idiopathic epiretinal membrane (iERM) and healthy controls who underwent OCT and OCTA examinations. The study was conducted from April 2025 to July 2026 at the Department of Ophthalmology, General Hospital of Central Theater Command.

2. Study participants and grouping

iERM cases were identified based on ophthalmic examination, OCT morphological features, and the Govetto staging criteria. Inclusion criteria for the case group were: (1) a diagnosis of iERM confirmed by BCVA, slit-lamp biomicroscopy, and OCT examinations, meeting the Govetto stages 1–4 criteria; (2) clear refractive media and the ability to cooperate with OCT and OCTA examinations; and (3) OCT image quality sufficient for staging and structural measurement.

Exclusion criteria for the case group were: (1) secondary epiretinal membrane (e.g., resulting from diabetic retinopathy, retinal vein occlusion, uveitis, or ocular trauma); (2) high myopia with a spherical equivalent (SE) > − 6.00 D or an axial length (AL) > 26 mm; (3) a history of intraocular surgery or retinal laser photocoagulation that could affect macular microcirculation; (4) systemic diseases affecting retinal blood flow (e.g., diabetes mellitus, uncontrolled hypertension, hematological disorders, or autoimmune diseases); and (5) other ocular diseases affecting the assessment of macular structure or microcirculation (e.g., age-related macular degeneration, macular hole, pathologic myopic maculopathy, or glaucoma).

Inclusion criteria for the healthy control group were: (1) intraocular pressure (IOP) of 10–21 mmHg; (2) a spherical equivalent between − 3.00 and + 3.00 D; (3) no iERM or other abnormalities affecting the macular structure or microcirculation on ophthalmic examination; and (4) no systemic diseases affecting retinal blood flow. The exclusion criteria for healthy controls were the same as items (2)–(5) of the case-group exclusion criteria.

Only one eye per participant was included in the study: for iERM patients with bilateral involvement, one eye was randomly selected as the study eye and the fellow eye was not included in the analysis. The final case group comprised 78 iERM eyes, classified by Govetto stage into 19 eyes in stage 1, 25 in stage 2, 19 in stage 3, and 15 in stage 4; the healthy control group comprised 25 eyes.

3. Clinical examination, OCT/OCTA acquisition, and quality control

All participants underwent BCVA, slit-lamp biomicroscopy, IOP, OCT, and OCTA examinations. Decimal visual acuity was converted to logMAR. The case and healthy control groups were examined using the same TOPI-SIGMA-1000 device, with the same scan area and the same scan protocol. Macular OCTA scans covered an area of 6 mm × 6 mm and were used to obtain central macular thickness (CMT), FAZ-related metrics, superficial VD, deep VD, and choroidal VD.

OCTA images were acquired by the same experienced technician. After acquisition, image quality was independently assessed by two trained investigators who were masked to the participants' clinical information and group assignment. Images included in the analysis had to meet the following criteria: (1) a signal strength index ≥ 6; (2) no significant motion artifacts (manifested as discontinuity of the vascular course, image distortion, or interlayer misalignment between adjacent B-scans); and (3) no significant projection artifacts interfering with the interpretation of the superficial and deep vascular plexuses. For images with minor artifacts, re-acquisition was performed on site, and the highest-quality image was ultimately selected for analysis.

Using the built-in automated segmentation algorithm of the device, the superficial capillary plexus (SCP) was defined as extending from the internal limiting membrane (ILM) to the outer boundary of the inner plexiform layer (IPL), and the deep capillary plexus (DCP) was defined as extending from the outer boundary of the IPL to the outer boundary of the outer plexiform layer (OPL). Given that contraction and traction of the epiretinal membrane can cause retinal folding and automated segmentation offsets, a senior investigator reviewed the automated segmentation results of all images layer by layer, and layers with erroneous boundaries were manually corrected before metric measurement.

4. Outcome measures and staging scheme

The primary outcomes were superficial and deep retinal VD in the 6 mm × 6 mm macular scan, and the interaction between iERM stage and vascular layer. Key secondary outcomes included CMT, FAZ perimeter, and FAZ circularity; other secondary structural metrics included FAZ area, FAZ-300 density, and FAZ fractal dimension. Choroidal VD was analyzed separately as a secondary blood-flow reference metric and was not part of the main superficial–deep retinal interaction.

iERM was classified into stages 1–4 according to the Govetto criteria. Stage 1 was characterized by a largely preserved foveal contour with the membrane appearing as a continuous hyperreflective line; stage 2 by loss of the foveal depression and widening of the outer nuclear layer; stage 3 by the additional

appearance of a continuous hyporeflective cleavage within the inner nuclear layer; and stage 4 by the further development of retinal pigment epithelium irregularities or marked disorganization of the full-thickness retinal structure.

5. Statistical analysis

Statistical analyses were performed using SPSS software (version 29.0). Continuous variables were presented as mean ± standard deviation or median (interquartile range) according to their distribution, and categorical variables as counts and percentages. Within the case group, linear mixed-effects models with the study eye as a random intercept were used to analyze iERM stage, vascular layer, and their interaction, thereby accounting for the correlation between superficial and deep VD measurements within the same eye; the healthy-reference analysis included healthy controls and iERM stages 1–4 in the same model, with adjustment for age and sex. CMT and FAZ-related metrics were analyzed using age- and sex-adjusted HC3 robust linear regression, and within-group stage trends were assessed using HC3 robust linear trend models. In iERM eyes, with logMAR BCVA as the outcome, unadjusted associations between nine imaging metrics and visual acuity were first evaluated using Spearman correlation analysis, followed by separate HC3 robust linear regression models incorporating age, sex, and categorical iERM stage to assess the imaging metric–visual acuity associations after adjustment for stage. Interactions were assessed using joint Wald χ^2 tests, and model results are reported as estimates or β coefficients, 95% confidence intervals, and P values. The Holm method was used for multiple-comparison correction in between-group comparisons, structural and blood-flow outcomes, and visual-acuity association analyses, respectively. Eye-level generalized estimating equations (GEE) were used only for sensitivity analysis and not as the primary basis for inference. All tests were two-sided, and $P < 0.05$ was considered statistically significant.

Results

1. Study population and data completeness

The dataset comprised 103 eyes of 103 participants, including 25 healthy control eyes and 78 iERM eyes. iERM stages 1–4 included 19, 25, 19, and 15 eyes, respectively; the participant screening flow and representative imaging findings for each iERM stage are shown in Fig. 1. The mean age was 53.64 ± 13.95 years in the healthy control group and 65.96 ± 11.66 years in the iERM group; the overall difference in age among the five groups was significant (Kruskal–Wallis $H = 18.53$, $P < 0.001$). Baseline characteristics and raw imaging metrics of all groups are shown in Table 1.

Table 1
Baseline characteristics and raw imaging metrics by group.

Metric	Healthy control (n = 25)	iERM stage 1 (n = 19)	iERM stage 2 (n = 25)	iERM stage 3 (n = 19)	iERM stage 4 (n = 15)	iERM overall (n = 78)
Age (years)	53.64 ± 13.95	67.47 ± 9.51	64.96 ± 13.77	66.74 ± 7.67	64.73 ± 14.96	65.96 ± 11.66
Sex (female/male, n)	14/11	12/7	10/15	12/7	8/7	42/36
BCVA (logMAR)	0.08 ± 0.11	0.53 ± 0.39	0.35 ± 0.19	0.54 ± 0.26	0.69 ± 0.27	0.50 ± 0.30
CMT (μm)	236.7 ± 21.5	264.9 ± 51.6	388.0 ± 42.7	463.2 ± 89.7	491.6 ± 143.4	396.3 ± 118.2
FAZ area (mm²)	0.338 ± 0.133	0.348 ± 0.158	0.211 ± 0.099	0.188 ± 0.067	0.217 ± 0.183	0.240 ± 0.141
FAZ perimeter (mm)	2.35 ± 0.57	2.56 ± 0.73	2.03 ± 0.65	1.73 ± 0.46	1.92 ± 0.67	2.06 ± 0.69
FAZ circularity	0.756 ± 0.087	0.659 ± 0.083	0.612 ± 0.127	0.568 ± 0.118	0.549 ± 0.103	0.601 ± 0.116
FAZ-300 density (%)	42.97 ± 3.82	39.36 ± 5.32	39.53 ± 3.05	39.81 ± 3.59	36.49 ± 4.90	38.97 ± 4.29
FAZ fractal dimension	1.051 ± 0.024	1.057 ± 0.018	1.092 ± 0.046	1.073 ± 0.025	1.064 ± 0.037	1.074 ± 0.037
Superficial VD (%)	41.44 ± 2.69	40.89 ± 2.69	39.56 ± 2.75	37.11 ± 2.69	37.53 ± 4.47	38.90 ± 3.41
Deep VD (%)	44.24 ± 1.39	43.26 ± 2.23	43.40 ± 1.94	41.21 ± 2.42	38.73 ± 4.40	41.94 ± 3.24
Choroidal VD (%)	49.92 ± 0.91	49.37 ± 1.57	49.48 ± 1.45	50.26 ± 2.47	49.33 ± 2.94	49.62 ± 2.09

Continuous variables are presented as mean ± standard deviation, and sex as female/male counts. iERM, idiopathic epiretinal membrane; CMT, central macular thickness; FAZ, foveal avascular zone; FAZ-300, vessel density within a 300-μm ring surrounding the FAZ; VD, vessel density; logMAR, logarithm of the minimum angle of resolution; SD, standard deviation.

2. Superficial and deep retinal VD within the case group

In the primary linear mixed-effects model for the case group, the joint Wald test for the iERM stage × vascular layer interaction yielded $\chi^2 = 7.21$, df = 3, P = 0.065, which did not reach the conventional threshold for statistical significance. The GEE sensitivity analysis yielded $\chi^2 = 8.32$, df = 3, P = 0.040,

indicating that the statistical evidence for the interaction was model-sensitive. In the primary model, estimated superficial VD decreased from 40.89% in stage 1 to 37.11% in stage 3, and deep VD decreased from 43.26% in stage 1 to 38.73% in stage 4 (Fig. 2).

Superficial VD was 3.79 percentage points lower in stage 3 than in stage 1 (95% CI, − 5.61 to − 1.97; Holm-adjusted P < 0.001), and 3.36 percentage points lower in stage 4 than in stage 1 (95% CI, − 5.30 to − 1.42; Holm-adjusted P < 0.001). Deep VD was 4.67 percentage points lower in stage 4 than in stage 2 (95% CI, − 6.50 to − 2.84; Holm-adjusted P < 0.001), and 4.53 percentage points lower in stage 4 than in stage 1 (95% CI, − 6.47 to − 2.59; Holm-adjusted P < 0.001) (Table 2). These results suggest that different vascular layers exhibit distinct stage-related patterns, although they cannot demonstrate the temporal sequence of the changes.

Table 2
Within-layer stage comparisons from the primary mixed-effects model of the case group.

Stage comparison	Difference (percentage points)	95% CI	Holm-adjusted P
Superficial VD: stage 3 vs. stage 1	−3.79	−5.61 to − 1.97	< 0.001
Superficial VD: stage 4 vs. stage 1	−3.36	−5.30 to − 1.42	< 0.001
Deep VD: stage 4 vs. stage 2	−4.67	−6.50 to − 2.84	< 0.001
Deep VD: stage 4 vs. stage 1	−4.53	−6.47 to − 2.59	< 0.001

Comparisons are within-layer stage contrasts from the primary linear mixed-effects model of the case group, with the Holm method applied for multiple-comparison correction. VD, vessel density; CI, confidence interval; iERM, idiopathic epiretinal membrane.

3. Retinal VD relative to healthy controls

In the five-group model including healthy controls and iERM stages 1–4, the unadjusted group × vascular layer interaction did not reach statistical significance ($\chi^2 = 8.82$, df = 4, P = 0.066); after adjustment for age and sex, the results remained essentially unchanged ($\chi^2 = 8.82$, df = 4, P = 0.066). In age- and sex-adjusted comparisons of each stage against healthy controls, neither superficial nor deep VD differed significantly between stage 1 and healthy controls; superficial VD in stage 2 was 1.83 percentage points lower than in healthy controls, with a Holm-adjusted P = 0.084. In stage 3, superficial and deep VD were 4.32 and 3.01 percentage points lower than in healthy controls (Holm-adjusted P < 0.001 and 0.002, respectively); in stage 4, superficial and deep VD were 3.88 and 5.48 percentage points lower, respectively (both Holm-adjusted P < 0.001). Clear reductions in VD relative to healthy levels were observed mainly in iERM stages 3–4 (Fig. 3).

4. Macular foveal structure and FAZ metrics

Raw distributions of macular foveal structural and FAZ metrics in each group are shown in Fig. 4. In the age- and sex-adjusted HC3 robust linear models, overall differences among the five groups (healthy controls and iERM stages 1–4) were significant for CMT, FAZ area, FAZ perimeter, FAZ circularity, FAZ-300 density, and FAZ fractal dimension (Holm-adjusted P < 0.001, < 0.001, < 0.001, < 0.001, 0.003, and 0.006, respectively). Choroidal VD showed no clear between-group differences (Holm-adjusted P = 0.212) (Table 3).

Within the case group, stage-trend analyses showed that CMT increased by 76.66 μm per stage (95% CI, 53.47 to 99.86; Holm-adjusted P < 0.001); FAZ perimeter decreased by 0.232 mm per stage (95% CI, − 0.384 to − 0.081; Holm-adjusted P = 0.013); and FAZ circularity decreased by 0.038 per stage (95% CI, − 0.059 to − 0.017; Holm-adjusted P = 0.002). The negative trend in FAZ area was not significant after Holm correction (β = −0.043; 95% CI, − 0.079 to − 0.007; Holm-adjusted P = 0.074), and FAZ-300 density, FAZ fractal dimension, and choroidal VD showed no clear linear stage trends (Table 4).

Table 3
Overall between-group tests for structural, FAZ, and choroidal VD metrics relative to healthy controls.

Outcome	Age/sex-adjusted overall test	Raw P	Holm-adjusted P
CMT	F(4, 96) = 82.89	< 0.001	< 0.001
FAZ area	F(4, 96) = 8.81	< 0.001	< 0.001
FAZ perimeter	F(4, 96) = 7.44	< 0.001	< 0.001
FAZ circularity	F(4, 96) = 11.46	< 0.001	< 0.001
FAZ-300 density	F(4, 96) = 5.08	< 0.001	0.003
FAZ fractal dimension	F(4, 96) = 4.28	0.003	0.006
Choroidal VD	F(4, 96) = 1.49	0.212	0.212

Overall between-group differences among healthy controls and iERM stages 1–4 were compared using HC3 robust linear regression adjusted for age and sex, with Holm correction. F, test statistic; CMT, central macular thickness; FAZ, foveal avascular zone; VD, vessel density; iERM, idiopathic epiretinal membrane.

Table 4
Linear stage trends for structural, FAZ, and choroidal VD metrics within the case group.

Outcome	Change per stage	95% CI	Holm-adjusted P
CMT	76.66	53.47 to 99.86	< 0.001
FAZ area	−0.043	−0.079 to − 0.007	0.074
FAZ perimeter	−0.232	−0.384 to − 0.081	0.013
FAZ circularity	−0.038	−0.059 to − 0.017	0.002
FAZ-300 density	−0.76	−1.83 to 0.31	0.485
FAZ fractal dimension	0.000	−0.007 to 0.007	1.000
Choroidal VD	0.10	−0.41 to 0.61	1.000

Linear changes per stage within the case group were analyzed using HC3 robust linear regression adjusted for age and sex, with Holm correction. CI, confidence interval; CMT, central macular thickness; FAZ, foveal avascular zone; VD, vessel density; iERM, idiopathic epiretinal membrane.

5. Associations between imaging metrics and visual acuity

In the 78 iERM eyes, unadjusted Spearman analysis showed that FAZ circularity was negatively correlated with logMAR (ρ = −0.364, P = 0.001; Holm-adjusted P = 0.010), as was deep VD (ρ = −0.319, P = 0.004; Holm-adjusted P = 0.036). The unadjusted P values for FAZ fractal dimension and choroidal VD were 0.025 and 0.045, respectively, but neither reached statistical significance after Holm correction. After further adjustment for age, sex, and categorical iERM stage, only FAZ circularity remained negatively associated with logMAR (β = −0.080 per 0.1 increase; 95% CI, − 0.133 to − 0.027; Holm-adjusted P = 0.029). The association between deep VD and logMAR was no longer significant after adjustment for stage (β = −0.048 per 5-percentage-point increase; 95% CI, − 0.176 to 0.080; Holm-adjusted P = 1.000). CMT, FAZ area, FAZ perimeter, FAZ-300 density, FAZ fractal dimension, superficial VD, and choroidal VD showed no stable associations with logMAR after adjustment (Table 5).

Table 5
Associations between imaging metrics and logMAR visual acuity in iERM eyes.

Imaging metric (regression unit)	Spearman ρ	Unadjusted P (Holm)	Adjusted β	Adjusted 95% CI	Adjusted P (Holm)
CMT (per 100 μm)	0.176	0.124 (0.619)	0.056	−0.025 to 0.137	0.175 (1.000)
FAZ area (per 1 mm²)	0.020	0.862 (1.000)	0.103	−0.426 to 0.632	0.702 (1.000)
FAZ perimeter (per 1 mm)	0.113	0.326 (0.977)	0.098	−0.013 to 0.210	0.084 (0.673)
FAZ circularity (per 0.1)	−0.364	0.001 (0.010)	−0.080	−0.133 to −0.027	0.003 (0.029)
FAZ-300 density (per 1 percentage point)	−0.158	0.166 (0.665)	−0.008	−0.023 to 0.008	0.324 (1.000)
FAZ fractal dimension (per 1 unit)	−0.253	0.025 (0.176)	−0.319	−1.945 to 1.308	0.701 (1.000)
Superficial VD (per 1 percentage point)	−0.073	0.525 (1.000)	−0.001	−0.020 to 0.019	0.953 (1.000)
Deep VD (per 5 percentage points)	−0.319	0.004 (0.036)	−0.048	−0.176 to 0.080	0.459 (1.000)
Choroidal VD (per 1 percentage point)	−0.228	0.045 (0.270)	−0.023	−0.053 to 0.007	0.127 (0.891)

Spearman correlations and regression analyses were performed in the 78 iERM eyes. Regression units were per 100 μm for CMT, per 0.1 for FAZ circularity, and per 5 percentage points for deep VD, with the remaining metrics analyzed in their raw units. A negative β indicates that a higher imaging metric was associated with a lower logMAR (better visual acuity). Values in parentheses are Holm-adjusted P values. FAZ, foveal avascular zone; VD, vessel density; CMT, central macular thickness; iERM, idiopathic epiretinal membrane; logMAR, logarithm of the minimum angle of resolution.

Discussion

1. Main findings

In this study, higher iERM stage was associated with thicker CMT and lower FAZ perimeter and circularity; compared with healthy controls, the reductions in superficial and deep VD were observed mainly in stages 3 and 4, whereas choroidal VD showed no stage-related change. Although the numeric trajectories of superficial and deep VD across stages differed slightly, the interaction between the two layers in the primary mixed-effects model was not significant (P = 0.065); this between-layer difference should therefore be regarded only as a trend, and it does not allow conclusions about the temporal sequence of blood-flow changes or the mechanism of disease progression. With regard to visual acuity,

FAZ circularity remained associated with worse logMAR visual acuity after adjustment for age, sex, and stage, whereas the association between deep VD and visual acuity disappeared after adjustment for stage, indicating that different imaging metrics carry different functional information.

2. Retinal VD and layer-specific patterns

Compared with healthy controls, no clear differences in superficial or deep VD were observed in iERM stages 1 and 2, whereas both layers were already below healthy levels by stages 3 and 4, suggesting that the more evident retinal microvascular abnormalities in this cohort were concentrated in the middle and late stages. Previous studies have also reported FAZ and retinal microvascular abnormalities in iERM, but their findings regarding the direction of superficial and deep VD changes and their relationship with structural severity are not entirely consistent, which may be attributable to differences in devices, scan areas, segmentation methods, and disease severity [16, 17].

3. Stage-related patterns of superficial and deep VD

Within the case group, the trajectories of superficial and deep VD across stages were not identical, and this study did not observe a significant interaction between superficial and deep VD, which is not fully consistent with the findings of Zhan et al., who focused on the nerve fiber layer plexus (NFLP) and ganglion cell layer plexus (GCLP); this discrepancy may be attributable to differences in scan area (6 × 6 mm versus 3 × 3 mm) and segmentation approach[20]. Although the GEE sensitivity analysis reached significance (P = 0.040), this in fact indicates that the conclusion is sensitive to model specification. Previous studies have shown that both the superficial and deep capillary plexuses may exhibit blood-flow abnormalities, although the extent of involvement and spatial distribution differ[21]. Preoperative–postoperative studies have further observed that ERM-related vascular parameters can undergo remodeling in parallel with changes in the inner retinal structure and tractional status[22]. Taken together, iERM may indeed show layer-specific differences in microvascular changes, but the current evidence is insufficient to determine whether superficial or deep blood-flow changes occur first.

4. Stage-related macular and FAZ structural changes

CMT increased with stage, by an average of approximately 76.66 μm per stage, whereas FAZ perimeter and circularity decreased with stage. Previous studies have indicated that the EIFL, disorganization of the retinal inner layers, and other foveal structural abnormalities are associated with iERM severity and visual functional decline[4–6], and foveal structural changes have also been considered to reflect the extent of macular tissue remodeling[7, 8]. The present study further supports a cross-sectional association between Govetto staging and foveal structural remodeling. The reductions in FAZ perimeter and circularity are consistent with geometric changes in the foveal vascular network caused by membrane traction; previous OCTA studies have also observed reduced FAZ area, distorted borders, and

extension of vessels toward the fovea in patients with iERM, and postoperative changes in FAZ morphology may occur[10, 15]. However, the linear stage trend of FAZ area within the case group was not significant after multiple-comparison correction, suggesting that different FAZ metrics reflect different structural dimensions and that FAZ changes are not necessarily simply linear. FAZ parameters should therefore be regarded as an integrated phenotype of foveal structure and vascular geometry rather than being interpreted solely as capillary ischemia.

5. Other vascular metrics and choroidal VD

Although FAZ-300 density and FAZ fractal dimension differed across the five groups in the overall comparison, neither showed a clear linear stage trend within the case group, suggesting that the relationship of these metrics with iERM stage may be nonlinear and that inter-individual variability is large. Previous studies have reported that metrics such as vascular skeleton density, vessel diameter, tortuosity, and fractal dimension are associated with iERM severity[17], and other studies have further examined the relationships of these microvascular parameters with macular sensitivity, visual acuity, and postoperative function[18, 19]. Choroidal VD showed no significant differences among healthy controls and iERM stages, and no clear stage trend was observed within the case group. This contrasts with the reduction in retinal VD in the middle and late stages, suggesting that the more evident blood-flow abnormalities in this cohort mainly involve the retinal microcirculation, while choroidal changes are minor or have not reached the level detectable with the present sample size. Previous studies suggest that iERM may be accompanied by changes in choroidal structural or vascular parameters, but their relationship with layer-specific retinal VD remains unclear[23]. Preoperative–postoperative studies have also observed changes in macular vascular circulation and retinal oxygen saturation[24, 25]. The choroidal VD results of the present study should therefore be regarded as a negative reference and cannot exclude a potential role of the choroidal microcirculation in iERM.

6. Associations between imaging metrics and visual acuity

In iERM eyes, lower FAZ circularity was associated with worse logMAR visual acuity, and this association persisted after adjustment for age, sex, and stage. Previous studies suggest that FAZ morphology and retinal vascular parameters may be associated with visual acuity[15–17], and deep capillary plexus VD may also be related to macular sensitivity [18]. However, other studies have shown that some FAZ and VD metrics do not exhibit stable postoperative prognostic value after incorporating clinical factors[19]. In the present study, deep VD was associated with visual acuity only without adjustment for stage, and this association disappeared after adjustment; CMT also showed no independent association with visual acuity after adjustment for stage. This suggests that the crude correlation between deep VD and visual acuity may be driven mainly by stage differences, whereas the relationship between FAZ circularity and current visual acuity is relatively more stable. Clinically, FAZ morphology can serve as a supplementary observation metric beyond OCT-based structural staging, helping to indicate potential visual differences

among patients with similar stages and informing the decision of whether additional functional assessments such as microperimetry are warranted; however, at the current stage it is not sufficient on its own for diagnosis, prognostic judgment, or treatment-timing decisions.

7. Limitations and future directions

This study has several limitations. First, the cross-sectional design can only describe the accompanying relationships between iERM stage and imaging metrics, and cannot determine the temporal sequence of structural and VD changes or establish a causal relationship between them. Second, the age distributions of the case and healthy control groups differed; although age and sex were adjusted for in the analyses, residual confounding and the limited sample size may still affect the stability of some interaction results. Third, quantitative OCTA results can be affected by signal strength, motion artifacts, projection artifacts, centration, segmentation errors, and algorithmic differences, and related reports also recommend that image quality, scan protocols, and segmentation methods be described as key quality-control items[26–28]. Recent consensus standards have further emphasized the consistency of OCTA image-quality assessment and exclusion criteria[29]. In addition, this study evaluated functional status mainly using logMAR visual acuity and did not incorporate microperimetry, metamorphopsia, or other more sensitive functional metrics. Future studies with larger samples, prospective longitudinal follow-up, standardized image quality control, and multidimensional visual function assessment are needed to further validate the functional significance of FAZ morphology and layer-specific VD.

Conclusions

This study demonstrated that iERM staging is associated with increased CMT, altered FAZ morphology, and reductions in superficial and deep retinal VD in the middle and late stages (relative to healthy levels). FAZ circularity remained associated with worse visual acuity even after adjustment for stage, suggesting that it may be a functionally relevant imaging feature beyond structural staging. Overall, OCTA can complement the characterization of the macular structural–microvascular phenotype of iERM; however, the present results are insufficient to infer the mechanism of disease progression or to determine the diagnostic and prognostic value of these metrics.

Abbreviations

AL: axial length

BCVA: best-corrected visual acuity

CMT: central macular thickness

DCP: deep capillary plexus

EIFL: ectopic inner foveal layer

FAZ: foveal avascular zone

GCLP: ganglion cell layer plexus

GEE: generalized estimating equations

iERM: idiopathic epiretinal membrane

ILM: internal limiting membrane

IOP: intraocular pressure

IPL: inner plexiform layer

logMAR: logarithm of the minimum angle of resolution

NFLP: nerve fiber layer plexus

OCT: optical coherence tomography

OCTA: optical coherence tomography angiography

OPL: outer plexiform layer

SCP: superficial capillary plexus

SE: spherical equivalent

VD: vessel density

Declarations

Ethics approval and consent to participate

This study was approved by the Ethics Review Committee of the General Hospital of Central Theater Command (approval number: [2026]198-01). The study was performed in accordance with the Declaration of Helsinki, and the requirement for informed consent was waived by the ethics committee.

Consent for publication

Not applicable.

Availability of data and materials

The datasets used and/or analysed during the current study are available from the corresponding author on reasonable request.

Competing interests

The authors declare that they have no competing interests.

Funding

This study was supported by the Hubei Provincial Health Science and Technology Project (No. WJ2025M091) and the Postdoctoral Scientific Research Foundation of General Hospital of Central Theater Command (No. 2025BSH070).

Authors' contributions

HH and XZ: Conceptualization, Data curation, Formal analysis, Investigation, Writing – original draft. MY, YY, ZH, and YS: Methodology, Supervision, Writing – review & editing. CP, LY, and SS: Investigation. MY: Funding acquisition. All authors read and approved the final manuscript.

Acknowledgements

Not applicable.

References

1. Bu SC, Kuijer R, Li XR, et al. Idiopathic epiretinal membrane. Retina. 2014;34(12):2317–35.
2. Fung AT, Galvin J, Tran T. Epiretinal membrane: a review. Clin Exp Ophthalmol. 2021;49(3):289–308.
3. Fraser-Bell S, Guzowski M, Rochtchina E, et al. Five-year cumulative incidence and progression of epiretinal membranes: the Blue Mountains Eye Study. Ophthalmology. 2003;110(1):34–40.
4. Govetto A, Lalane RA 3rd, Sarraf D, et al. Insights into epiretinal membranes: presence of ectopic inner foveal layers and a new optical coherence tomography staging scheme. Am J Ophthalmol. 2017;175:99–113.
5. Doguizi S, Sekeroglu MA, Ozkoyuncu D, et al. Clinical significance of ectopic inner foveal layers in patients with idiopathic epiretinal membranes. Eye (Lond). 2018;32(10):1652–60.
6. Zur D, Iglicki M, Feldinger L, et al. Disorganization of retinal inner layers as a biomarker for idiopathic epiretinal membrane after macular surgery: the DREAM Study. Am J Ophthalmol. 2018;196:129–35.
7. Govetto A, Bhavsar KV, Virgili G, et al. Tractional abnormalities of the central foveal bouquet in epiretinal membranes: clinical spectrum and pathophysiological perspectives. Am J Ophthalmol.

2017;184:167–80.

8. Mahmoudzadeh R, Israilevich R, Salabati M, et al. Pars plana vitrectomy for idiopathic epiretinal membrane: OCT biomarkers of visual outcomes in 322 eyes. Ophthalmol Retina. 2022;6(4):308–17.
9. Okawa Y, Maruko I, Kawai M, et al. Foveal structure and vasculature in eyes with idiopathic epiretinal membrane. PLoS ONE. 2019;14(4):e0214881.
10. Muftuoglu IK, Amador M, Meshi A, et al. Foveal avascular zone distortion in epiretinal membrane by optical coherence tomography angiography. Ophthalmic Surg Lasers Imaging Retina. 2019;50(5):295–301.
11. Chen H, Chi W, Cai X, et al. Macular microvasculature features before and after vitrectomy in idiopathic macular epiretinal membrane: an OCT angiography analysis. Eye (Lond). 2019;33(4):619–28.
12. Mao J, Xu Z, Lao J, et al. Assessment of macular microvasculature features before and after vitrectomy in idiopathic macular epiretinal membrane using a grading system: an optical coherence tomography angiography study. Acta Ophthalmol. 2021;99(7):e1168–75.
13. Bacherini D, Dragotto F, Caporossi T, et al. The role of OCT angiography in the assessment of epiretinal macular membrane. J Ophthalmol. 2021;2021:8866407.
14. Ulfik-Dembska K, Teper S, Dembski M, et al. Idiopathic epiretinal membrane: microvasculature analysis with optical coherence tomography and optical coherence tomography angiography. Tomography. 2022;8(1):189–99.
15. Ersoz MG, Hocaoglu M, Sayman Muslubas I, et al. Quantitative assessment of the foveal avascular zone using optical coherence tomography angiography before and after surgery for idiopathic epiretinal membrane. Retina. 2021;41(1):54–9.
16. Kim YJ, Kim S, Lee JY, et al. Macular capillary plexuses after epiretinal membrane surgery: an optical coherence tomography angiography study. Br J Ophthalmol. 2018;102(8):1086–91.
17. Hsia Y, Hsieh YT. Associations between macular retinal vasculature and severity of idiopathic epiretinal membrane. BMC Ophthalmol. 2023;23(1):200.
18. Feng J, Yang X, Xu M, et al. Association of microvasculature and macular sensitivity in idiopathic macular epiretinal membrane: using OCT angiography and microperimetry. Front Med (Lausanne). 2021;8:655013.
19. Henry M, Ndiaye NC, Angioi-Duprez K et al. Association of microvasculature changes with visual outcomes in idiopathic epiretinal membrane surgery: a clinical trial. J Clin Med. 2024;13(16).
20. Zhan J, Zhang Q, Yang J, et al. Layer-specific microvascular changes in idiopathic epiretinal membrane: implications for visual function. Retina. 2026;46(4):604–12.
21. Coppe AM, Lapucci G, Gilardi M, et al. Alterations of macular blood flow in superficial and deep capillary plexuses in the fellow and affected eyes of patients with unilateral idiopathic epiretinal membrane. Retina. 2020;40(8):1540–8.

22. Mao J, Lao J, Liu C, et al. A study analyzing macular microvasculature features after vitrectomy using OCT angiography in patients with idiopathic macular epiretinal membrane. BMC Ophthalmol. 2020;20(1):165.
23. Wang X, Yang J, Wang C, et al. Choroidal morphologic and vascular features in patients with unilateral idiopathic epiretinal membranes: an optical coherence tomography analysis integrated with assessment of retinal layers. Front Med (Lausanne). 2022;9:1083601.
24. Li Z, Zhang J, Lin T, et al. Macular vascular circulation and retinal oxygen saturation changes for idiopathic macular epiretinal membrane after vitrectomy. Acta Ophthalmol. 2019;97(3):296–302.
25. Isik-Ericek P, Sizmaz S, Esen E, et al. The effect of epiretinal membrane surgery on macular microvasculature: an optical coherence tomography angiography study. Int Ophthalmol. 2021;41(3):777–86.
26. Borrelli E, Parravano M, Sacconi R, et al. Guidelines on optical coherence tomography angiography imaging: 2020 focused update. Ophthalmol Ther. 2020;9(4):697–707.
27. Sampson DM, Dubis AM, Chen FK, et al. Towards standardizing retinal optical coherence tomography angiography: a review. Light Sci Appl. 2022;11(1):63.
28. Al-Sheikh M, Ghasemi Falavarjani K, Akil H, et al. Impact of image quality on OCT angiography based quantitative measurements. Int J Retina Vitreous. 2017;3:13.
29. Wicklein R, Yam C, Noll C, et al. The OSCAR-MP consensus criteria for quality assessment of retinal optical coherence tomography angiography. Neurol Neuroimmunol Neuroinflamm. 2023;10(6):e200149.

Figures

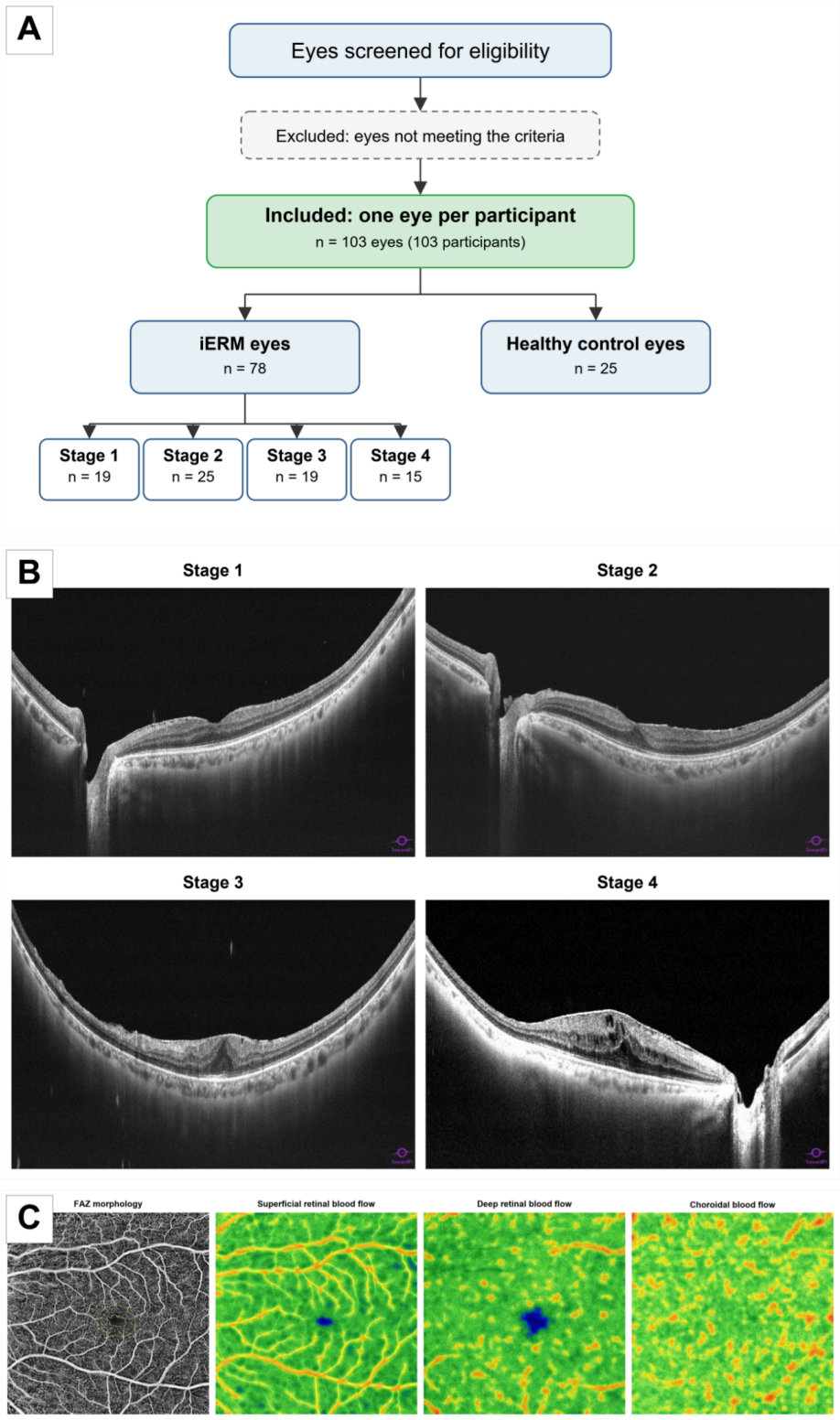


Figure 1

Study population and representative imaging findings of iERM at different stages. A: Study flow of 103 single-eye datasets. B: Representative OCT images of iERM at different stages. C: Representative OCTA images of iERM at different stages.

Figure 2. Stage-associated retinal VD by vascular layer

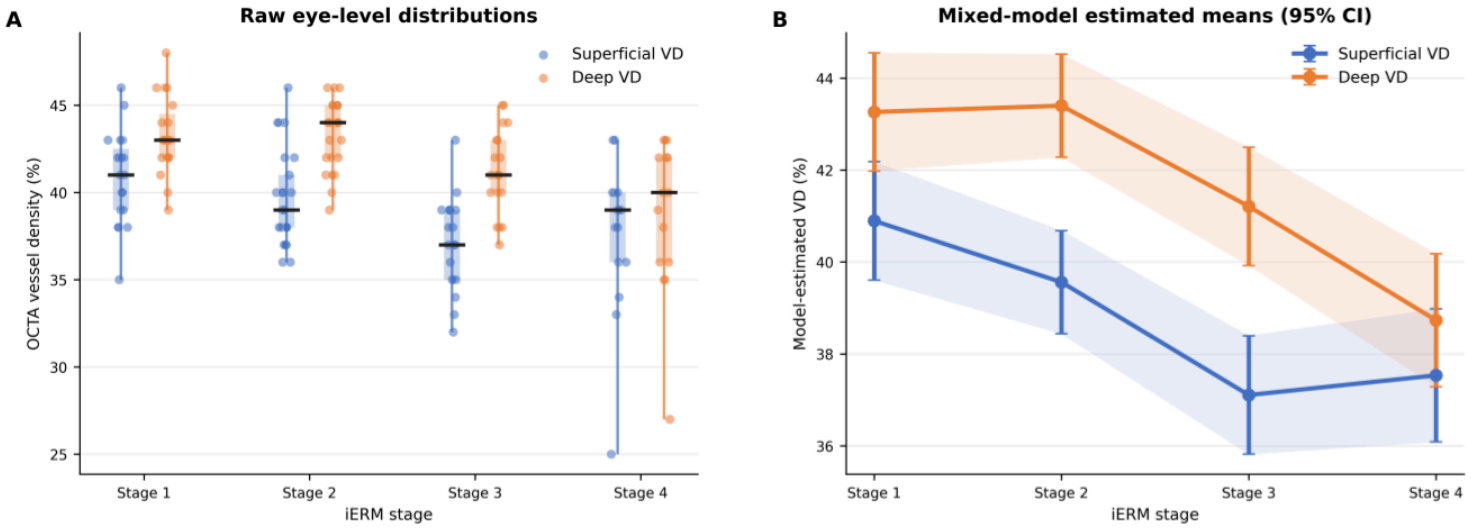


Figure 2

Layer-specific retinal VD results by iERM stage. A: Eye-level raw distributions of superficial and deep VD. B: Estimated marginal means and 95% CIs from the primary linear mixed-effects model. The primary interaction was $\chi^2 = 7.21$, df = 3, P = 0.065; the GEE sensitivity analysis was $\chi^2 = 8.32$, df = 3, P = 0.040.

Figure 3. Age/sex-adjusted retinal VD differences versus healthy controls

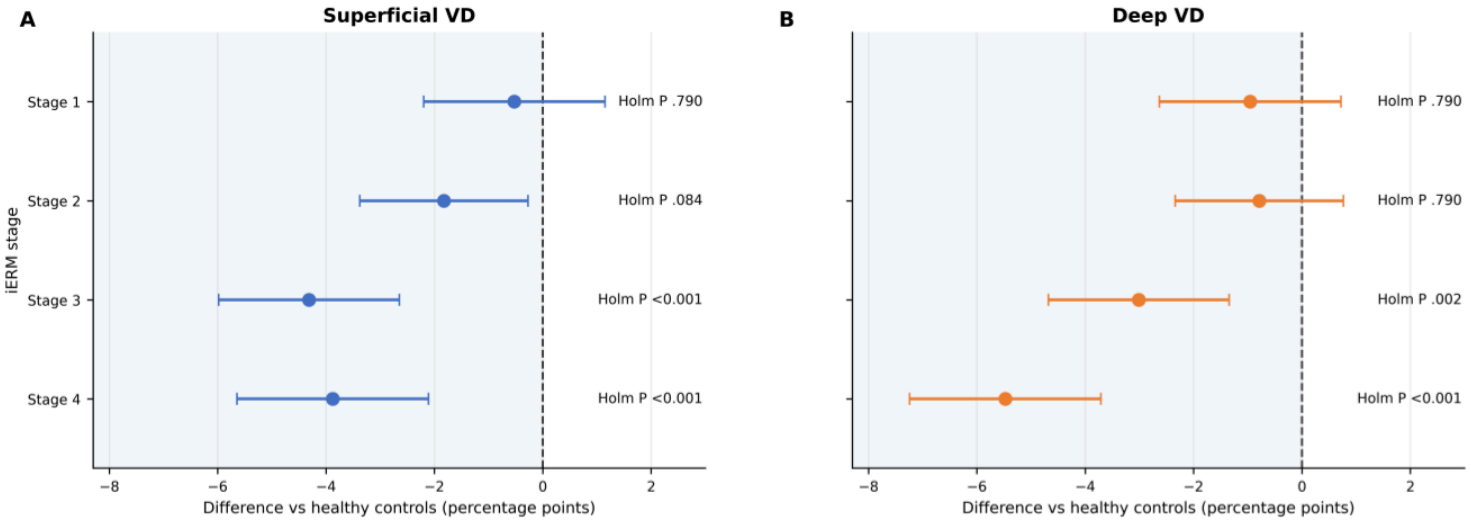


Figure 3

Age- and sex-adjusted retinal VD differences relative to healthy controls. A: Superficial VD. B: Deep VD. Points and horizontal lines represent adjusted differences and nominal 95% CIs; the dashed line indicates zero difference; negative values indicate lower VD in the iERM group than in healthy controls. P values were corrected by the Holm method.

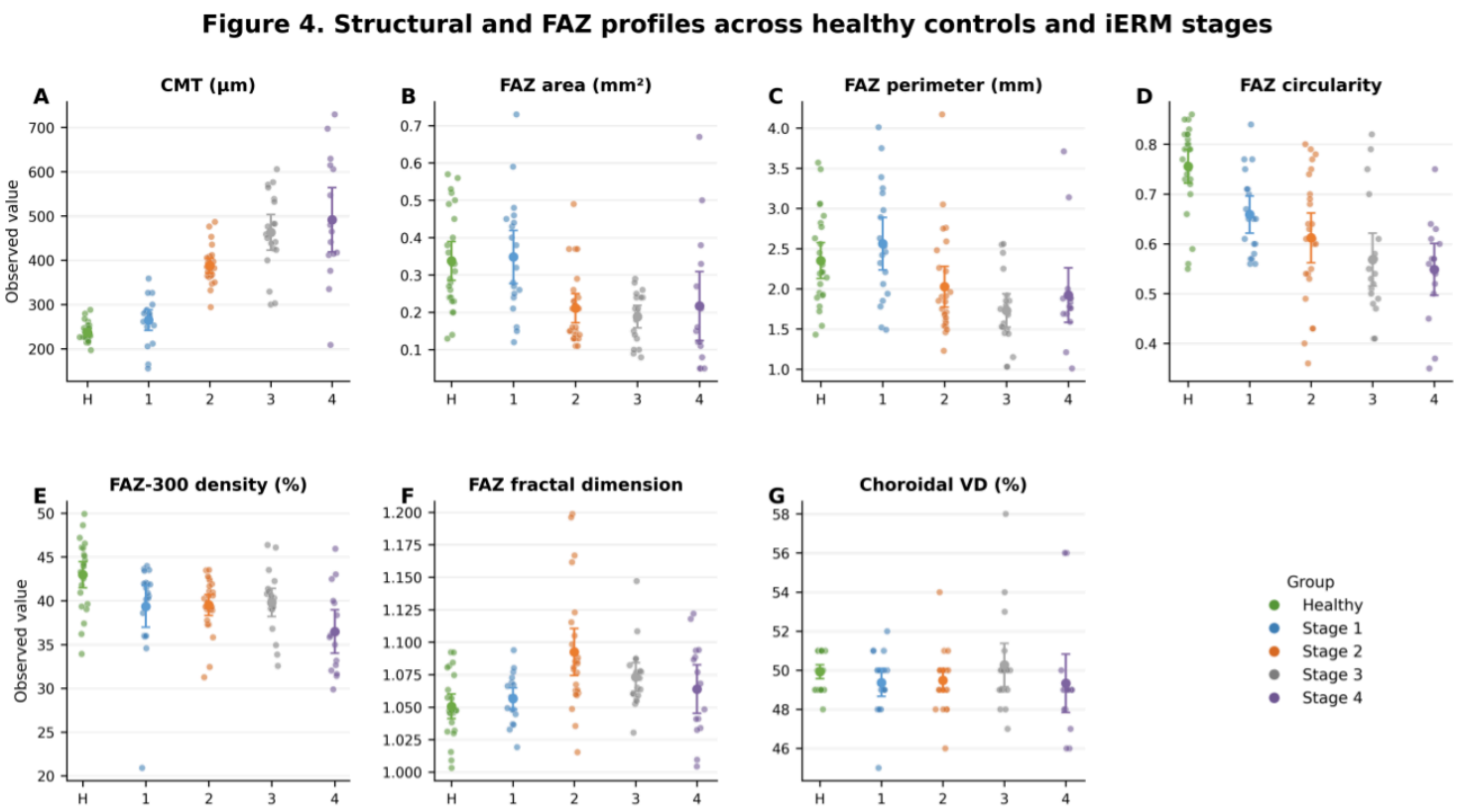


Figure 4

Raw distributions of structural and FAZ metrics in healthy controls and different iERM stages. Dots represent individual-eye observations; colored circles and error bars represent group means and 95% CIs. H indicates healthy controls and 1–4 indicate iERM stages.